INVERSE DETERMINATION OF AEROHEATING AND CHARRING ABLATOR RESPONSE

Jeremie B.E. Meurisse, Science and Technology Corporation at NASA Ames Research Center (jeremie.b.meurisse@nasa.gov)
Nagi N. Mansour, NASA Ames Research Center (nagi.n.mansour@nasa.gov)

IPPW-2018, June
University of Colorado Boulder
Abstract number: 679

Introduction

The Mars Science Laboratory (**MSL**) was protected during its Mars atmospheric entry by an instrumented heatshield that used NASA's Phenolic Impregnated Carbon Ablator (**PICA**) [1]. PICA is a lightweight carbon fiber/polymeric resin material that offers excellent performances for protecting probes during planetary entry. The Mars Entry Descent and Landing Instrument (**MEDLI**) suite on MSL offers unique in-flight validation data for models of atmospheric entry and material response. MEDLI recorded, among others, time-resolved in-depth temperature data of PICA using thermocouple sensors assembled in the MEDLI Integrated Sensor Plugs (**MISP**). These measurements have been widely used in the literature as a validation benchmark for state-of-the-art ablation codes [2,3,4]. The objective of this work is to perform an inverse estimate of the MSL heatshield material properties and aerothermal environment during Mars entry from the MISP **flight data**.

Inverse estimation methodology

The inverse problem is handled by the **DAKOTA** library [12]. A multi-objective genetic algorithm and a trust-region method for nonlinear least squares are used to estimate key uncertain material parameters that influence the material response model. We follow the strategy of Mahzari et al [2,3] by using first the thermocouple driver approach to estimate uncertain parameters of the material model (**TC1 driver**). In this case, the temperature is imposed at the location of the shallowest MISP thermocouple. Then, the **aerothermal environment** is estimated by fitting the in-depth measured thermocouple response flight measurements. Finally, the laminar and turbulent environments from the Data Parallel Line Relaxation Code (DPLR) [11] are compared to the inverse solutions. This work represents an important milestone toward the development of validated **predictive capabilities** for designing Thermal Protection Systems for planetary probes.

NASA Release
DPLR: https://software.nasa.gov/software/ARC-16021-1A
PATO: https://software.nasa.gov/software/ARC-16680-1

Porous material Analysis Toolbox based on OpenFOAM (PATO)

The computational model is a generic mass and heat transfer model for porous reactive materials containing several solid phases and a single gas phase. The detailed chemical interactions occurring between the solid phases and the gas phase are modeled at the pore scale assuming Local Thermal Equilibrium (**LTE**). This model is implemented in the Porous material Analysis Toolbox based on OpenFOAM (**PATO**) [5,6,7], a C++ top level module of the open source computational fluid dynamics software program **OpenFOAM**. The open source third party library **Mutation++**, produced by the von Karman Institute for Fluid Dynamics, is dynamically linked to compute equilibrium chemistry compositions and thermodynamic and transport properties [8]. For this study, the Theoretical Ablative Composite for Open Testing (TACOT) database developed by the TPS community was used to define the porous material properties. TACOT is a fictitious material that was inspired from low density carbon/phenolic ablators.

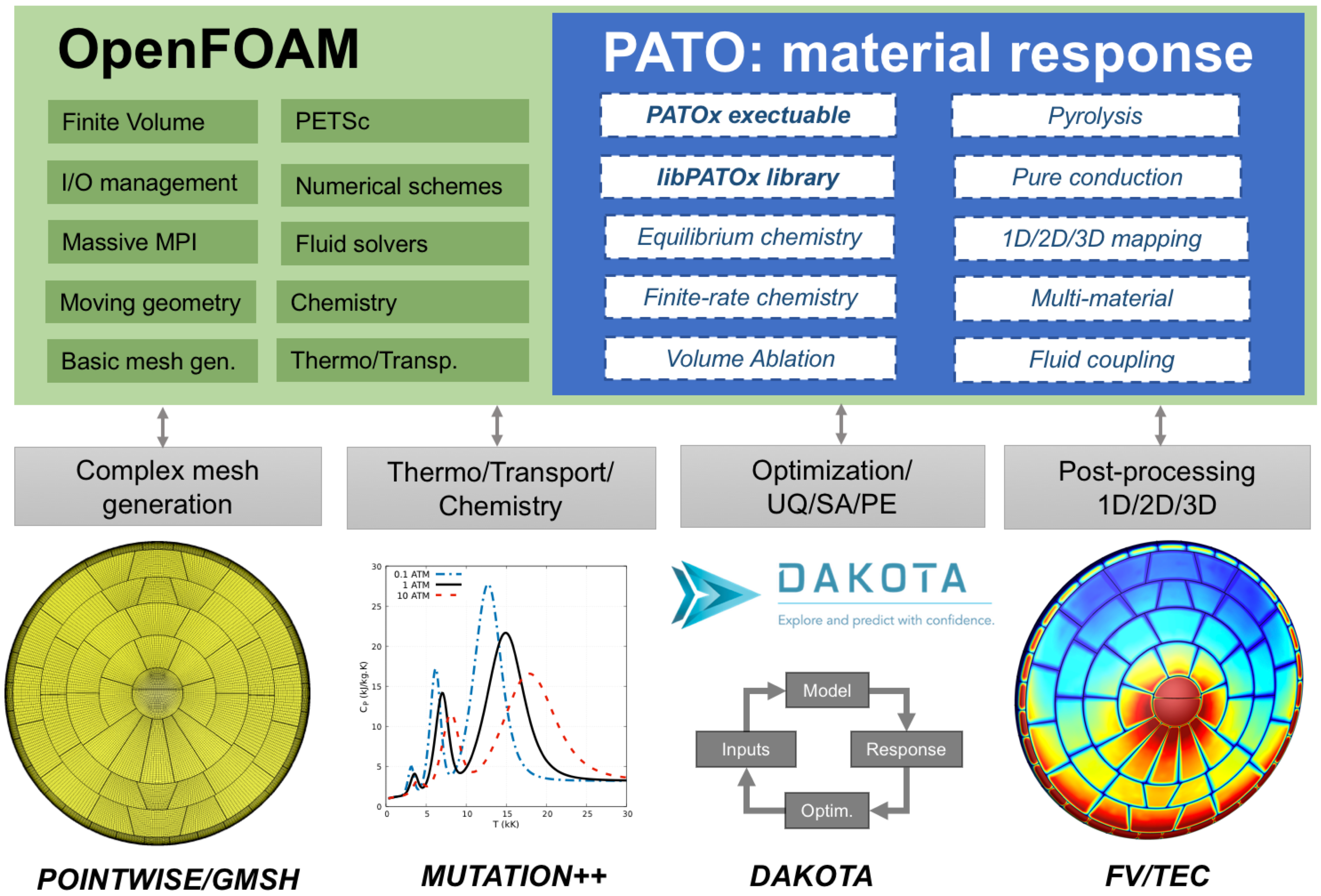

Fig. 1 Software architecture of the Porous material Analysis Toolbox based on OpenFOAM (PATO) version 3

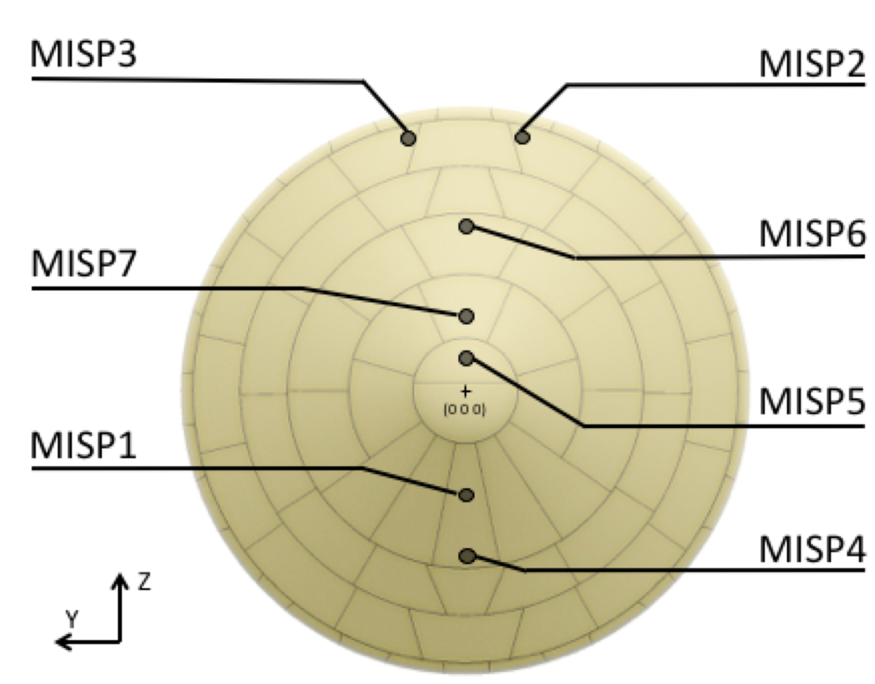

Fig. 2 MEDLI Integrated Sensor Plug (MISP) [7]

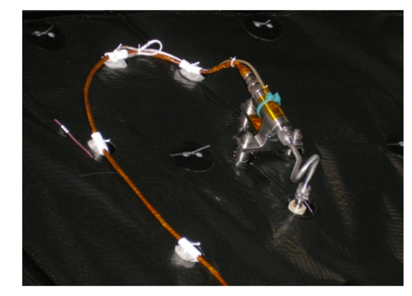

Fig. 3 MEADS pressure sensor [13]

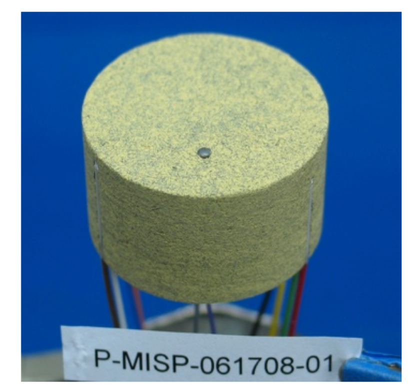

Fig. 4 MISP [13]

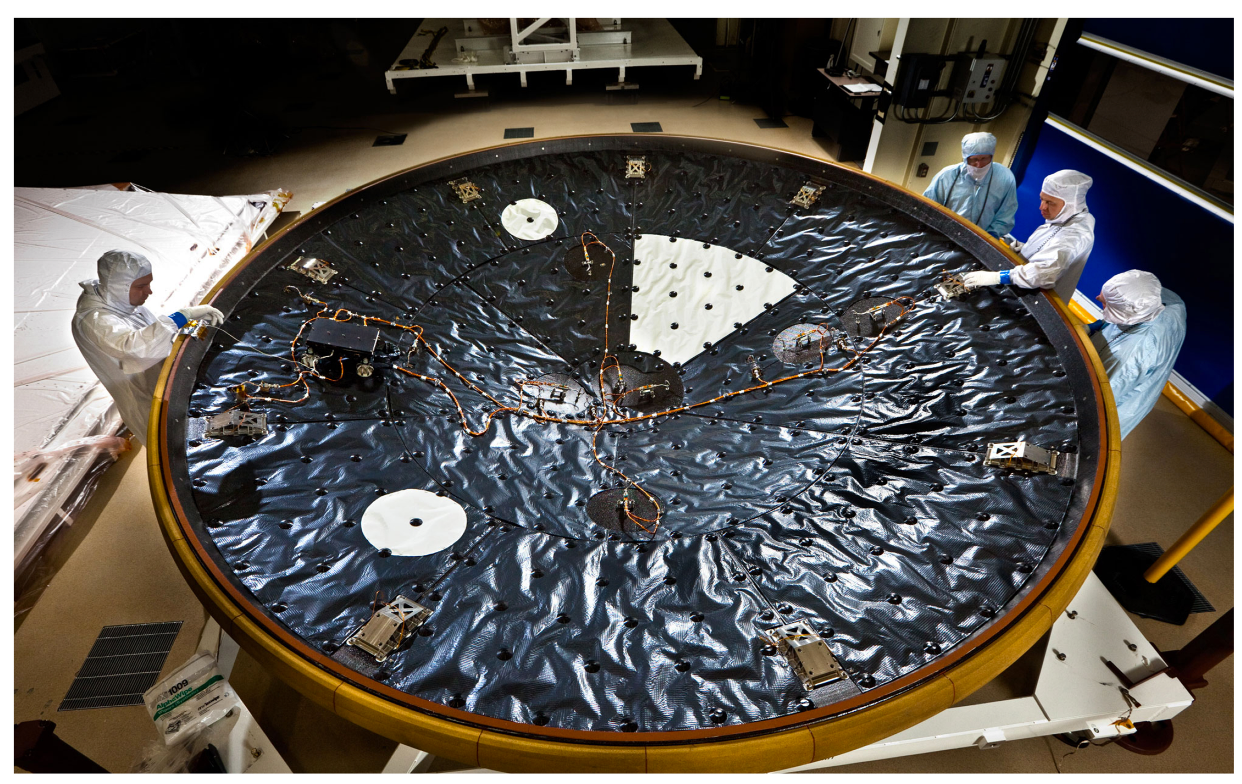

Fig. 5 MSL EDL Instrument (MEDLI) Suite assembling [13]

TC1 driver results

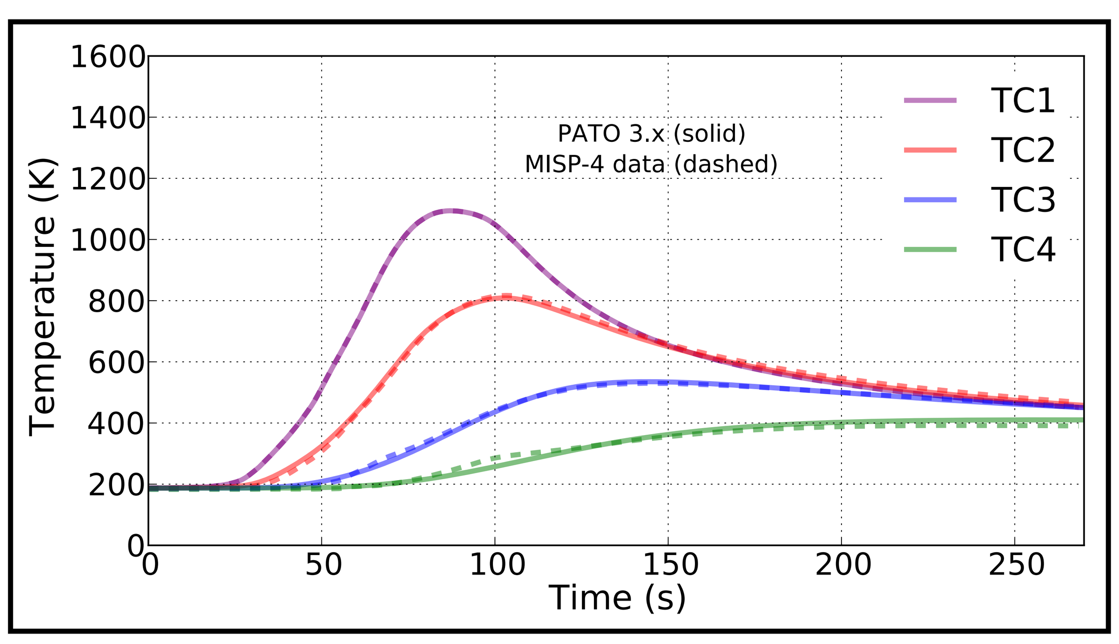

Fig. 6 Thermal response at MISP4 using TC1 driver

- **Estimation of material properties**
- Shallowest MISP 4 thermocouple
- Imposed wall temperature
- Equilibrium chemistry [7]
- Calibrated pyrolysis [9]
- TC4 hump due to water [10]

Inverse environment results

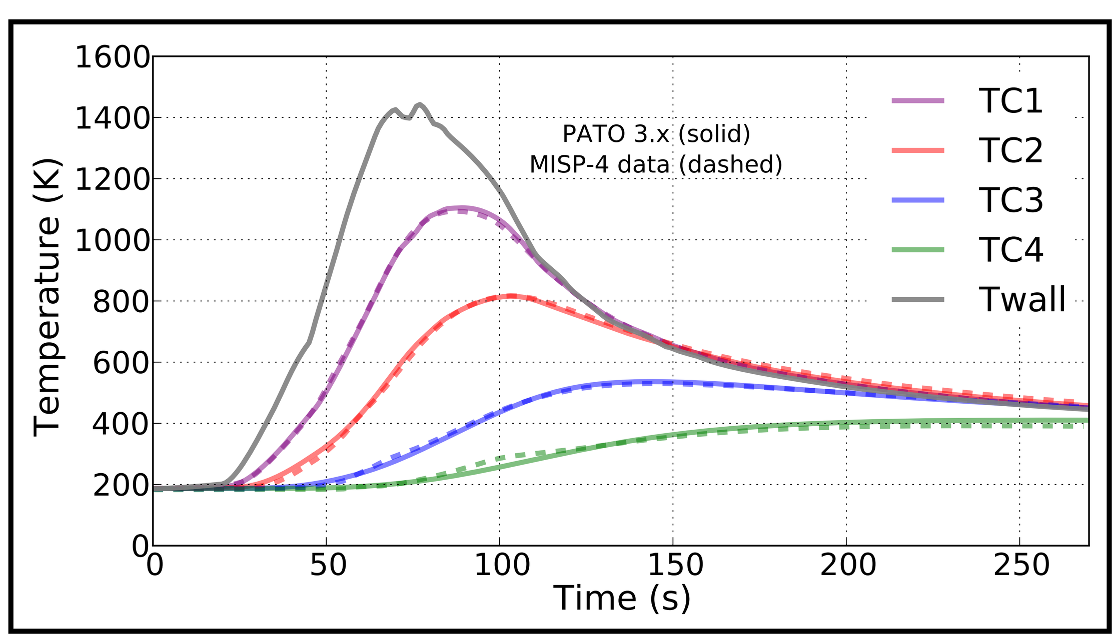

Fig. 7 Thermal response at MISP4 using the inverse environment

- **Estimation of surface convective heat flux and char ablation rate**
- Calculated temperature and recession using surface mass and energy balance
- Material properties from TC1 driver
- Note oscillations of wall temperature

Comparison to DPLR results

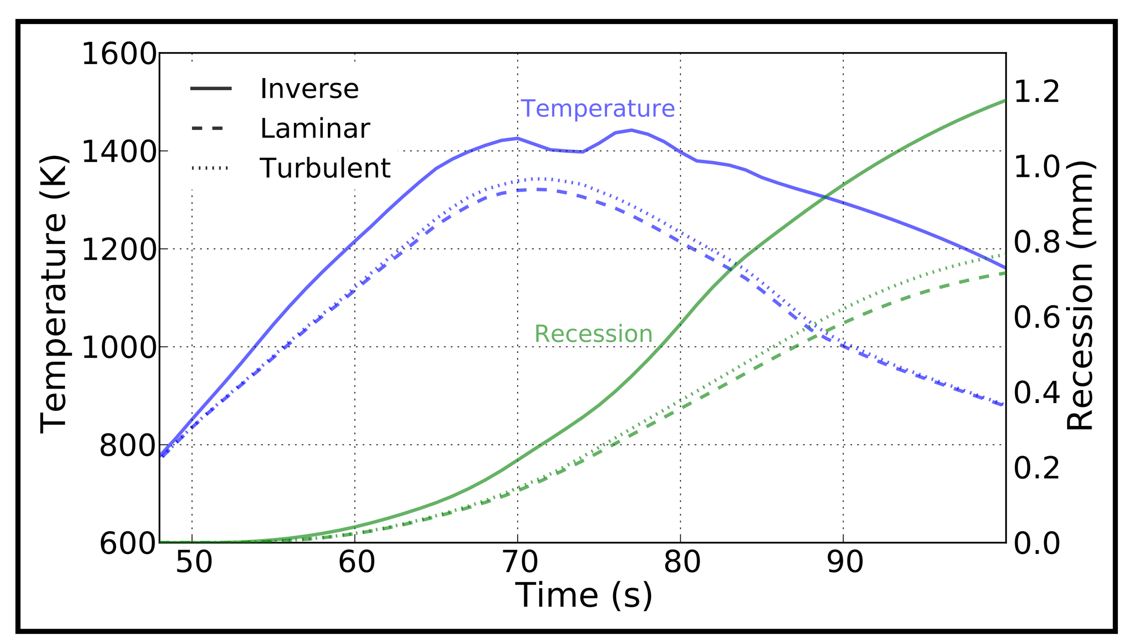

Fig. 8 Inverse and DPLR environment results

- **Comparison of inverse derived environment with laminar and turbulent DPLR derived aerothermal environments**
- DPLR environment underestimate temperature and recession at stag. point

References

[1] M.J. Wright et al. (2009), *AIAA Paper*, 2009-423.
[2] M. Mahzari et al. (2013), *PhD Diss., Georgia Institute of Technology*.
[3] M. Mahzari et al. (2015), *Journal of Spacecraft and Rockets*, 52.4, 1203-1216.
[4] T.R. White et al. (2013), *AIAA Paper*, 2013-2779.
[5] J. Lachaud and N. N. Mansour (2014), *J Thermophys Heat Tran,* 28, 191–202.
[6] J. Lachaud et al. (2017), *Int J Heat Mass Tran*, 108, 1406–1417.
[7] J. B.E. Meurisse et al. (2018), *Aerosp Sci Technol*, 76, 497-511.
[8] J. B. Scoggins and T. E. Magin (2014), *AIAA Paper,* 2014-2966.
[9] F. Torres (2017), *Ablation Workshop*.
[10] A.D. Omidy et al. (2016), *Journal of Thermophysics and Heat Transfer,* 473-478.
[11] M.J. Wright et al. (2009), *DPLR Code User Manual*.
[12] SANDIA (2014), https://dakota.sandia.gov/documentation.html, 05/15/18.
[13] NASA, https://mars.nasa.gov/msl/mission/instruments/atmossensors/medli, 05/15/18.